

# Dynamic transition embedding for image feature extraction and recognition

Zhihui Lai · Zhong Jin · Jian Yang ·  
Mingming Sun

Received: 11 November 2010 / Accepted: 21 March 2011  
© Springer-Verlag London Limited 2011

**Abstract** In this paper, we propose a novel method called dynamic transition embedding (DTE) for linear dimensionality reduction. Differing from the recently proposed manifold learning-based methods, DTE introduces the dynamic transition information into the objective function by characterizing the Markov transition processes of the data set in time  $t(t > 0)$ . In the DTE framework, running the Markov chain forward in time, or equivalently, taking the larger powers of Markov transition matrices integrates the local geometry and, therefore, reveals relevant geometric structures of the data set at different timescales. Since the Markov transition matrices defined by the connectivity on a graph contain the intrinsic geometry information of the data points, the elements of the Markov transition matrices can be viewed as the probabilities or the similarities between two points. Thus, minimizing the errors of the probability reconstruction or similarity reconstruction instead of the least-square reconstruction in the well-known manifold learning algorithms will obtain the optimal linear projections with respect to preserving the intrinsic Markov processes of the data set. Comprehensive comparisons and extensive experiments show that DTE achieves higher recognition rates than some well-known linear dimensionality reduction techniques.

**Keywords** Manifold learning · Dimensionality reduction · Feature extraction · Markov transition matrix · Dynamic transition processes

## 1 Introduction

Recent research showed that many high-dimensional data in real world applications are usually lie on or near a low-dimensional manifold embedded in a high-dimensional space. In order to make the high-dimensional data more suitable for further process, it is very important to discover and faithfully preserve the intrinsic geometry structure of the raw data on dimensionality reduction. The goal of dimensionality reduction is to map the high-dimensional data to a lower-dimensional subspace in which certain geometric properties of interest are preserved.

The classical linear dimensionality reduction techniques include principle component analysis (PCA) [1, 2, 4, 5] and linear discriminant analysis (LDA) [3–5]. However, PCA and LDA fail to discover the underlying nonlinear manifold structure and cannot preserve the local geometry. In order to overcome the drawbacks in these linear methods and deal with the nonlinear data, the kernel extension of the linear methods, i.e., kernel principle component analysis (KPCA) [6] and kernel linear discriminant analysis (KLDA) [7], have been proposed and attracted much attention in the fields of pattern recognition and machine learning. In recent years, there have been great interest in geometry-based nonlinear manifold learning, and many nonlinear techniques have been proposed. The representative methods include isomap [8], locally linear embedding (LLE) [9], Laplacian eigenmap (LE) [10, 11], local tangent space alignment (LTSA) [12], and diffusion maps [13]. Isomap tries to preserve the global topological structure, i.e., geodesic distance, of the original data when the data are mapped onto a lower-dimensional subspace, whereas LLE tries to unfold the manifold by preserving the local linear reconstruction relationship of the data. LE tries to preserve the local nearest neighborhood relationship,

---

Z. Lai (✉) · Z. Jin · J. Yang · M. Sun  
School of Computer Science, Nanjing University  
of Science and Technology, 210094 Nanjing, Jiangsu,  
People's Republic of China  
e-mail: lai\_zhi\_hui@163.com

whereas HLLC [14] modifies LE by estimating the *Hessian* instead of the *Laplacian* on the manifold. LTSA captures the internal global coordinates of the data points by aligning a set of local tangent spaces. Unlike LE and LLE, diffusion maps try to preserve the diffusion distance in the low-dimensional subspace by performing a *random walk* on the data and calculating the eigenvectors of the transition matrix as the low-dimensional coordinates. In addition, the recently developed Riemannian manifold learning algorithm [15] tries to learn the Riemannian manifold structure by preserving distances and angles between each pair of samples.

Although these nonlinear methods have yielded impressive results on artificial and real world data sets, they can not give explicit maps and how to evaluate the maps on new test data points remains unclear. As a result, these nonlinear manifold learning methods might not be suitable for some tasks, such as face and palm-print recognition. A nature way to obtain the explicit maps is to perform the linear approximations of the nonlinear dimensionality reduction techniques, which include neighborhood preserving embedding (NPE) [16], locality preserving projections (LPP) [17], and linear local tangent space alignment (LLTSA) [18]. These linear extension methods aim to find a low-dimensional linear subspace on which the corresponding geometry manners can be maximally preserved. PCA seeks a subspace to preserve the variance of the data set. LDA is a supervised learning algorithm that searches a set of projections on which both the between-class separability and the within-class compactness are maximized. NPE, the linear extension of LLE, aims to preserve the local neighborhood reconstructive relationship in a linear subspace. LPP, a linear extension of LE, attempts to preserve the relative location relationships in each local neighborhood of the data set. LLTSA preserves the essential manifold structure by linearly approximating the local tangent space coordinates.

By integrating the local neighborhood information and class label information together, local discriminant embedding (LDE) [19], marginal Fisher analysis (MFA) [20], discriminant simplex analysis (DSA) [21], constrained maximum variance mapping (CMVM) [22], and some 2D/kernel variants [23–25] are also developed to enhance the performances in feature extraction and classification. In fact, most of these manifold learning-based methods, no matter supervised or unsupervised methods, use the same graph-embedding framework [20], i.e., unnormalized graph Laplacian, for feature extraction. However, since the data set are usually nonuniform distribution, the frequently used unnormalized graph Laplacian is not suitable for manifold learning-based algorithms when compared with normalized graph Laplacian [26–29].

In this paper, we proposed a new linear method named dynamic transition embedding (DTE) for linear dimensionality reduction. Differing from the state-of-the-art manifold learning methods, DTE introduces the dynamic transition probability information of the Markov chain evolved forward in time into the objective function and preserves the dynamic probabilistic transition information in the low-dimensional subspace in any time  $t$ . The elements in the Markov transition matrices in any time can be viewed as the similarities or the transition probabilities between two points. We propose to minimize the errors of the probability reconstruction or similarity reconstruction instead of the least-square reconstruction in the well-known LLE or NPE. Thus, a novel geometric property is preserved in the low-dimensional subspace. To our best knowledge, there is no previously known method with such similar properties on linear dimensionality reduction.

The following properties should be highlighted in the proposed framework:

- The projections are designed to maximize a new objective criterion based on a probability transition processes or random walk on a graph, which is significantly different from the existing linear dimensionality reduction techniques.
- Unlike most manifold-based methods that use unnormalized Laplacian, DTE uses normalized graph Laplacian to model the probability transition processes.
- The discriminative ability and robustness of DTE are superior to classical linear dimensionality methods, such as PCA, LPP, NPE, and LLTAS. Therefore, DTE may be more suitable for dimensionality reduction in applications.

The rest of the paper is organized as follows. In Sect. 2, some related linear dimensionality reduction techniques are reviewed. DTE algorithm is described in Sect. 3. In Sect. 4, experiments are carried out to evaluate the proposed algorithm, and the experimental results are presented. Finally, the conclusions are given in Sect. 5.

## 2 A brief review of PCA, LPP, and NPE

Let matrix  $X = [x_1, x_2, \dots, x_N]$  be the data matrix, including all the training samples  $\{x_i\}_{i=1}^N \in R^m$  in its columns. In practice, the feature dimension  $m$  is often very high. The goal of the linear dimensionality reduction is to transform the data from the original high-dimensional space to a low-dimensional subspace, i.e.,

$$y = A^T x \in R^d \quad (1)$$

for any  $x \in R^m$  with  $d \ll m$ , where  $A = (\alpha_1, \alpha_2, \dots, \alpha_d)$  and  $\alpha_i (i = 1, \dots, d)$  is an  $m$ -dimensional column vector.

### 2.1 Principle component analysis (PCA)

PCA [1] preserves the global geometric structure, i.e., global scatter, of data in a transformed low-dimensional space. With the linear transformation in (1), the objective function of PCA is to maximize the global scatter of the samples:

$$\begin{aligned}
 J_{\text{PCA}} &= \sum_{i=1}^N \|y_i - \bar{y}\|^2 = \sum_{i=1}^N \|A^T(x_i - \bar{x})\|^2 \\
 &= \sum_{i=1}^N \text{tr}\{A^T(x_i - \bar{x})(x_i - \bar{x})^T A\} \\
 &= \text{tr}\{A^T S_T A\}
 \end{aligned}$$

where  $\bar{y} = \frac{1}{N} \sum_{i=1}^N y_i$ ,  $\bar{x} = \frac{1}{N} \sum_{i=1}^N x_i$ , and  $S_T$  is the total scatter matrix with  $S_T = \sum_{i=1}^N (x_i - \bar{x})(x_i - \bar{x})^T$ . The optimal projections of PCA are the first  $d$  generalized eigenvectors of the eigenfunction

$$S_T \alpha = \lambda \alpha \tag{2}$$

Since PCA only focuses on the global scatter, the local geometric structure of the data set may not be preserved in the learned subspace.

### 2.2 Locality preserving projections (LPP)

Unlike PCA, LPP aims to preserve the local geometric structure of the data set. The objective function of LPP is defined as follows:

$$\begin{aligned}
 \min \frac{1}{2} \sum_i \sum_j W_{ij}^{\text{LPP}} \|y_i - y_j\|^2 &= \min \text{tr}(A^T X \\
 &\times (D^{\text{LPP}} - W^{\text{LPP}}) X^T A)
 \end{aligned} \tag{3}$$

where  $y_i = A^T x_i$  ( $i = 1, \dots, N$ ),  $D_{ii}^{\text{LPP}} = \sum_j W_{ij}^{\text{LPP}}$ , and the affinity weight matrix  $W^{\text{LPP}}$  is defined as

$$W_{ij}^{\text{LPP}} = \begin{cases} \exp(-\|x_i - x_j\|^2 / 2\varepsilon), & \text{if } x_i \in N_k(x_j) \text{ or } x_j \in N_k(x_i) \\ 0, & \text{otherwise} \end{cases}$$

where  $N_k(x_i)$  denotes the  $k$ -nearest neighbors of  $x_i$  and  $\varepsilon$  denotes the Gaussian kernel parameter.

By imposing a constraint of  $A^T X D^{\text{LPP}} X^T A = I$ , the optimal projections of LPP are given by the first  $d$  smallest nonzero eigenvalue solutions to the following generalized eigenvalue problem:

$$X(D^{\text{LPP}} - W^{\text{LPP}})X^T \alpha = \lambda X D^{\text{LPP}} X^T \alpha \tag{4}$$

where  $\alpha$  is a column vector of  $A$ .

Minimizing (3) means that if two points are close to each other in the original space, then they should be kept close in the low-dimensional transformed space. Thus, it is

obvious that LPP is effective for preserving the local neighborhood relationship of the data points of the underlying manifold.

### 2.3 Neighborhood preserving embedding (NPE)

NPE aims at preserving the local neighborhood geometric structure of the data. The affinity weight matrix of NPE is obtained from the coefficients of local least-square approximation. The local approximation error in NPE is measured by minimizing the cost function:

$$\sum_i \left\| x_i - \sum_{j \in \pi_k(x_i)} \omega_{ij} x_j \right\|^2 \tag{5}$$

where  $\pi_k(x_i)$  denotes the index set of  $k$ -nearest neighbors of  $x_i$ , and  $\omega_{ij}$ 's are the optimal local least-square reconstruction coefficients. The criterion for choosing an optimal projection  $\alpha$  is to minimize the cost function:

$$\begin{aligned}
 \sum_i \left\| \alpha^T x_i - \sum_{j \in \pi_k(x_i)} \omega_{ij} \alpha^T x_j \right\|^2 \\
 = \text{tr}(A^T X (I - W^{\text{NPE}})^T (I - W^{\text{NPE}}) X^T A)
 \end{aligned} \tag{6}$$

where  $W_{ij}^{\text{NPE}} = \omega_{ij}$ .

By removing an arbitrary scaling factor, the optimal projections of NPE are the eigenvectors corresponding to the minimum eigenvalue of the following generalized eigenvalue problem:

$$X(I - W^{\text{NPE}})^T (I - W^{\text{NPE}}) X^T \alpha = \lambda X X^T \alpha \tag{7}$$

As can be seen from (5 and 6), a drawback of NPE is that one should perform local least-square reconstruction for each point to obtain the weighted matrix  $W^{\text{NPE}}$ . Thus, NPE is relatively time consuming when compared with LPP. But NPE preserves the local reconstruction relationship of the data set, which is different from LPP.

### 3 Dynamic transition embedding (DTE)

In the literatures, many locality-based or manifold learning-based linear dimensionality methods [10, 11, 17, 19, 20, 22] usually, firstly, construct graphs to model the data structure and then linearly approximate the structure of the manifold. The unnormalized graph Laplacian is frequently used in these methods. However, since the data points are generally not uniformly distributed, Lafon et al. [26, 27] showed that the limit operator contains an additional drift term and they suggested a different kernel normalization on

Laplacian operator that separates the manifold geometry from the distribution of points on it. They also showed that normalized graph Laplacian could also recover the Laplace–Beltrami operator. Based on the theoretic analysis, Hein et al. [28] argued against using the unnormalized graph Laplacian. Luxburg [29] also suggested using the normalized graph Laplacian by evaluating their experimental results. These theorems and experiments show that the normalized graph Laplacian is more suitable for graph-based manifold learning algorithms.

In this paper, we use the normalized graph Laplacian and view them as the probability transition matrix of the Markov chain of the data set since the sum of each row of the matrix is equal to 1. The elements in the Markov transition matrix in any time can be viewed as the similarities or the transition probabilities between two points. We propose to minimize the errors of the probability (similarity) reconstruction instead of the least-square reconstruction in the well-known LLE or NPE. Then, the transition processes in any time  $t$  are preserved in the low-dimensional subspace. Thus, the learned subspace preserves a novel geometric property, which is significantly different from the existing linear dimensionality reduction method.

### 3.1 Learning the probability transition Markov matrix

Let us consider a set of  $N$  samples  $X = [x_1, x_2, \dots, x_N]$ , taking values in an  $m$ -dimensional Euclidean space. We define a pair-wise similarity matrix  $W$  between points, for example using a Gaussian kernel with width  $\varepsilon$  defined in the local neighborhood of the data set

$$W_{ij} = \begin{cases} \exp\left(-\frac{\|x_i - x_j\|^2}{2\varepsilon}\right), & \text{if } x_i \in N_k(x_j) \text{ or } x_j \in N_k(x_i) \\ \beta, & \text{otherwise.} \end{cases} \quad (8)$$

where  $N_k(x_i)$  denotes the data points in the first  $k$ -nearest neighbors of  $x_i$ , and  $\beta (\beta \in [0, 1])$  is a constant set by user. The elements in  $W$  measure the local connectivity of the data points and hence capture the local geometry of the data set. When the data points are out of the local neighborhood, the similarities are viewed as a constant, which simply characterize the nonlocal connections of the data set. Thus,  $W$  can be viewed as the local neighborhood graph defined on the data set. Let  $D$  be the diagonal matrix with the diagonal elements  $D_{ii} = \sum_j W_{ij}$ , and we can construct the following symmetric matrix

$$M_s = D^{-1/2} W D^{-1/2} \quad (9)$$

As it was mentioned in the literatures [10, 11, 13],  $D$  is an approximation of the true density of the data set. The symmetric matrix  $M_s$  is an anisotropic kernel that approximates the Fokker–Planck operator defined on the data set [30]. We normalize the anisotropic kernel  $M_s$ , and define the stochastic transition Markov matrix  $P = \bar{D}^{-1} M_s$  in time  $t$  as

$$P^t = (\bar{D}^{-1} M_s)^t \quad (10)$$

where the diagonal element of the diagonal matrix  $\bar{D}$  is defined as  $\bar{D}_{ii} = \sum_j M_{s,ij}$ .

Denote the entry of matrix  $P^t$  in the location  $(i, j)$  as  $p_t(x_i, x_j)$ , then  $p_t(x_i, x_j)$  can be interpreted as the probability of transition from  $x_i$  to  $x_j$  in time  $t$ . The quantity  $p_1(x_i, x_j)$  for  $t = 1$  reflects the first-order neighborhood structure of the graph [13]. Since  $P^t$  for any  $t > 0$  is still a Markov transition matrix, the new idea introduced in the proposed framework is to capture information on local neighborhoods by taking powers of the matrix  $P$  or equivalently to run the random walk forward in time. Increasing  $t$  corresponds to propagate the local influence of each node with its neighbors. That is, running the chain forward in time, or equivalently, taking larger powers of  $P$  will allow us to integrate the local geometry and, therefore, will reveal relevant geometric structures of  $X$  at different timescales.

### 3.2 Preserving the dynamic transition processes in linear subspace

In Sect. 1, we have mentioned that NPE aims to preserve the local neighborhood reconstructive relationship on the manifold, and LPP attempts to preserve the relative location relationship in each local neighborhood of the data set. Different from the NPE and LPP, DTE preserves another geometric property of the data set in a similar way with LLE and NPE. That is, Markov probability transition processes within the data set at any time  $t > 0$  are preserved in the low-dimensional subspace. Let  $y_1, y_2, \dots, y_N$  be the corresponding data points of  $x_1, x_2, \dots, x_N$  in the low-dimensional subspace. The objective function of DTE is to minimize the cost function of the probability transition processes in any time  $t$ :

$$\sum_i \left\| y_i - \sum_j p_t(x_i, x_j) y_j \right\|^2 \quad (11)$$

Since we want to obtain an optimal transformation matrix  $A$  such that  $y_i = A^T x_i$  ( $i = 1, \dots, N$ ), then from (11), we have

$$\begin{aligned} & \sum_i \left\| A^T x_i - \sum_j p_t(x_i, x_j) A^T x_j \right\|^2 \\ &= \sum_i \left( A^T x_i - \sum_j p_t(x_i, x_j) A^T x_j \right) \\ & \quad \times \left( A^T x_i - \sum_j p_t(x_i, x_j) A^T x_j \right)^T \\ &= \text{tr} \left( A^T X (I - P^t)^T (I - P^t) X^T A \right) \end{aligned} \tag{12}$$

Clearly, the matrix  $X(I - P^t)^T (I - P^t) X^T$  is symmetric and semi-positive definite. Similar to NPE, in order to remove an arbitrary scaling factor in the projection, we impose a constraint as follows:

$$\alpha^T X X^T \alpha = 1 \tag{13}$$

Finally, the minimization problem reduces to finding the optimal projection vector  $\alpha$ :

$$\arg \min_{\alpha^T X X^T \alpha = 1} \alpha^T X (I - P^t)^T (I - P^t) X^T \alpha \tag{14}$$

By using the Lagrange multiplier method, it is easy to show that the transformation vector  $\alpha$  that minimizes the objective function is given by the minimum eigenvalue solution to the following generalized eigenvector problem:

$$X (I - P^t)^T (I - P^t) X^T \alpha = \lambda X X^T \alpha \tag{15}$$

The optimal transformation matrix  $A_{DTE}$  is composed by the eigenvectors corresponding to the minimum eigenvalue solutions of (15).

Clearly, the significant difference between the NPE and the proposed DTE is that NPE preserves the local reconstruction relationship of the data set, and DTE preserves the dynamic transition processes of the data set in low-dimensional subspace instead. Moreover, the quantity  $p_t(x_i, x_j)$  has another physical interpretation. Since  $0 \leq p_t(x_i, x_j) \leq 1$  and  $\sum_j p_t(x_i, x_j) = 1$ ,  $p_t(x_i, x_j)$  directly shows us that how much percent information are transited from  $x_i$  to  $x_j$ . Since the reconstruction coefficients in LLE or NPE may be negative or positive (even bigger than 1), they cannot give such interpretations. Thus, DTE preserves the different geometric property, which potentially makes it perform much better than NPE.

### 3.3 The algorithm

It should be noted that the matrix  $XX^T$  in (15) might be singular, which stems from the small sample size problem. In order to overcome the complication of a singular matrix  $XX^T$ , we first project the data set to a PCA subspace so that the resulting matrix  $XX^T$  is nonsingular. Another consideration

of using PCA as preprocessing is for noise reduction. The preprocessing must be performed when we encounter the case mentioned earlier. Therefore, the final transformation matrix  $A$  can be expressed as follows:

$$A = A_{PCA} A_{DTE} \tag{16}$$

The DTE algorithmic procedures can be summarized as follows:

- Step1: Project the original data into the PCA subspace by throwing away the smallest principal components to overcome the singular problem.
- Step2: Compute the distance matrix between any two data points and construct an undirected graph  $W$  on  $X$  with a weight function defined in (8).
- Step3: Construct symmetric matrix  $M_s$  and Markov transition matrix  $P$ .
- Step4: Compute the optimized resolutions by solving the generalized eigenvalue problem based on (15) with a fixed time parameter  $t$  set by user.
- Step5: Project samples to the DTE subspace and adopt a suitable classifier for classification.

### 3.4 Kernel extension

In the proposed algorithm, a linear transformation is taken to improve the generalization ability. It is well known that in the kernel space, the generalization ability is also very powerful in some cases. Although we mainly focus on the linear method in this paper, we extend the proposed method with kernel trick and present the main processes for the special users who need to use the nonlinear techniques. To begin with, supposed the data is mapped into an implicit feature space  $H$  using a nonlinear function

$$\phi : x_i \in R^m \rightarrow \phi(x_i) \in H \tag{17}$$

Then, in the feature space, we would like to minimize

$$\begin{aligned} & \sum_i \left\| A^T \phi(x_i) - \sum_j p_t(\phi(x_i), \phi(x_j)) A^T \phi(x_j) \right\|^2 \\ &= \sum_i \left( A^T \phi(x_i) - \sum_j p_t(\phi(x_i), \phi(x_j)) A^T \phi(x_j) \right) \\ & \quad \times \left( A^T \phi(x_i) - \sum_j p_t(\phi(x_i), \phi(x_j)) A^T \phi(x_j) \right)^T \\ &= \text{tr} \left( A^T K (I - P^t_\phi)^T (I - P^t_\phi) K A \right) \end{aligned} \tag{18}$$

where  $K = \phi(X)^T \phi(X)$  is a kernel matrix, whose entries are  $K(i, j) = (\phi(x_i), \phi(x_j))$  and



**Fig. 1** Sample images of one person in the Yale database

$$W_{\phi,ij} = \begin{cases} \exp\left(-\frac{\|\phi(x_i) - \phi(x_j)\|^2}{2\epsilon}\right), & \text{if } \phi(x_i) \in N_k(\phi(x_j)) \text{ or } \phi(x_j) \in N_k(\phi(x_i)), \\ \beta, & \text{otherwise.} \end{cases}$$

$$D_{\phi,ii} = \sum_j W_{\phi,ij}, \quad M_{s\phi} = D_{\phi}^{-1/2} W_{\phi} D_{\phi}^{-1/2},$$

$$\bar{D}_{\phi,ii} = \sum_j M_{s\phi,ij}, \quad P_{\phi}^t = \left(\bar{D}_{\phi}^{-1} M_{s\phi}\right)^t$$

With a constraint of

$$A^T K K A = I \tag{19}$$

one can easily get the following generalized eigenvalue problem

$$K \left( I - P_{\phi}^t \right)^T \left( I - P_{\phi}^t \right) K \alpha = \lambda K K \alpha \tag{20}$$

and the matrix  $A$  is determined by the eigenvectors corresponding to the smallest  $d$  nonzero eigenvalues of (20). Once transformation matrix  $A$  is obtained, the high-dimensional data can be mapped into a  $d$ -dimensional subspace by

$$y = A^T \phi(x) = A^T [k(x_1, x), k(x_2, x), \dots, k(x_N, x)]^T \tag{21}$$

where  $k(\cdot, \cdot)$  is the kernel function set by user.

### 4 Experiments

To evaluate the proposed DTE algorithm, we compare it with the well-known unsupervised linear dimensionality reduction algorithms, i.e., PCA (Eigenface), LPP (Laplacianface), NPE and LLTSA on Yale, AR face databases, PolyU FKP, and NIR database [31–33]. The Yale database was used to examine the performance when both facial expressions and illumination are varied. The AR database was employed to test the performance of these methods

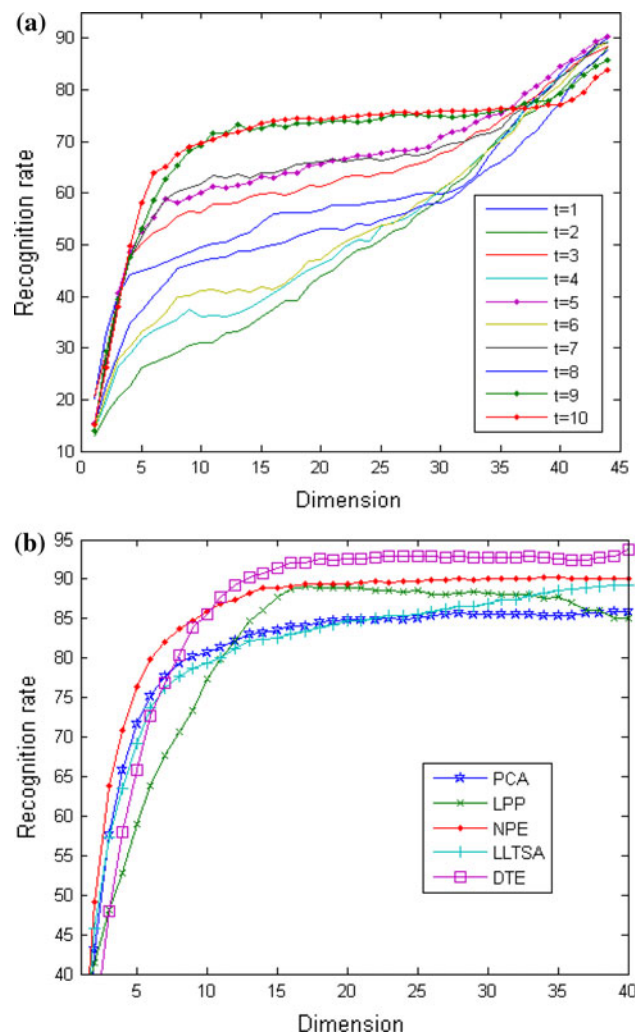


**Fig. 2** **a** The variations of recognition rates versus  $t$ . **b** The average recognition rates (%) versus the dimensions when 5 images per person were randomly selected for training and the remaining for test on the Yale face database

**Table 1** The maximal average recognition rates (percent) of five methods on the Yale database and the corresponding dimensions when 3, 4, 5, and 6 samples per class are randomly selected for training and the remaining for test

#/class	3	4	5	6
PCA	81.47(40) $\pm$ 3.83	85.26(37) $\pm$ 3.21	85.96(40) $\pm$ 1.79	86.93(34) $\pm$ 2.03
LPP	85.97(24) $\pm$ 3.35	88.57(21) $\pm$ 2.74	89.00(18) $\pm$ 2.03	90.40(21) $\pm$ 1.89
NPE	86.23(39) $\pm$ 3.27	89.01(33) $\pm$ 2.65	90.24(35) $\pm$ 2.13	91.33(32) $\pm$ 2.26
LLTSA	84.88(40) $\pm$ 3.67	86.59(40) $\pm$ 2.82	89.24(39) $\pm$ 2.47	90.13(37) $\pm$ 1.74
DTE	90.27(38) $\pm$ 2.31	92.43(38) $\pm$ 2.12	93.67(40) $\pm$ 1.41	94.91(40) $\pm$ 0.97

**Fig. 3** Sample images of one subject of the AR database. The first line and the second line images were taken in different time (separated by 2 weeks)

under conditions where there was a variation over time, in facial expressions and in lighting conditions. The FKP database was used to evaluate the performance when the images were captured in different time section. The NIR face database was used to test the performance of different methods on near-infrared face image recognition with variations of pose, expression, focus, scale, and time. The nearest neighbor classifier with Euclidean distance was used in all the experiments.

#### 4.1 Experiments on Yale database

The Yale face database contains 165 images of 15 individuals (each person providing 11 different images) under various facial expressions and lighting conditions. In our experiments, each image was manually cropped and resized to  $100 \times 80$  pixels. Figure 1 shows sample images of one person. For computational effectiveness, we down sample it to  $50 \times 40$  in this experiment.

In order to decide the optimal parameter  $t$ , we select 3 images per person for training and the remaining for test in the experiment. We ran the experiments for 10 times. The variations of recognition rates versus  $t$  are shown in Fig. 2a. As can be seen from the figure, the optimal parameter  $t$  is  $t = 5$  on this database.

In the experiments,  $l$  images ( $l$  varies from 3 to 6) are randomly selected from the image gallery of each individual to form the training sample set. The remaining  $11 - l$  images

are used for testing. For each  $l$ , we independently run the system 50 times. PCA, LPP, NPE, LLTSA, and DTE are, respectively, used for feature extraction. In the PCA phase of LPP, NPE, LLTSA, and DTE, the number of principle components is set as 40, kept about 96% of the image energy. The maximal average recognition rate of each method and the corresponding dimension are given in Table 1. The average recognition rates (%) versus the dimensions when 5 images per person were randomly selected for training and the remaining for testing is shown in Fig. 2b.

As it is shown in Table 1 and Fig. 2b, the top recognition rate of DTE is significantly higher than the compared methods. Why can DTE significantly outperform the other algorithms? An important reason may be that DTE not only characterizes the local geometry structure but also discovers the intrinsic relationships hidden within the data points at a certain time  $t$  steps by introducing dynamic processes, thus eliminates more negative influence of the variations of expressions and illuminations.

#### 4.2 Experiments on the AR face database

The AR face database contains over 4,000 color face images of 126 people (70 men and 56 women), including frontal views of faces with different facial expressions, lighting conditions, and occlusions. The pictures of 120 individuals (65 men and 55 women) were taken in two sessions (separated by 2 weeks), and each section contains

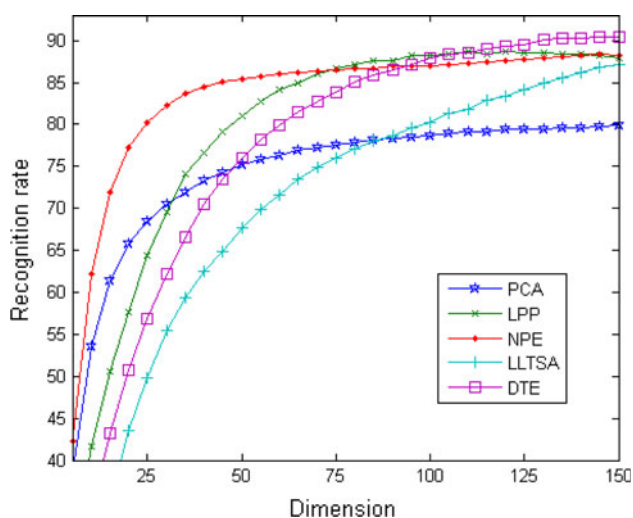


**Fig. 4** The average recognition rates (%) versus the dimensions when 5 images per person were randomly selected for training and the remaining for test on the AR face database

13 color images. 7 images of these 120 individuals are selected and used in our experiments. The face portion of each image is manually cropped and then normalized to  $50 \times 40$  pixels. The sample images of one person are shown in Fig. 3. These images vary as follows: 1. neutral expression; 2. smiling; 3. angry; 4. screaming; 5. left light on; 6. right light on; 7. all sides light on; 8. wearing sun glasses; 9. wearing sun glasses and left light on; and 10. wearing sun glasses and right light on.

In this experiment,  $l$  images ( $l$  varies from 2 to 6) are randomly selected from the image gallery of each individual to form the training sample set. The remaining  $20 - l$  images are used for test. For each  $l$ , we independently run the

algorithms 10 times. PCA, LPP, NPE, LLTSA, and DTE are, respectively, used for feature extraction. In the PCA phase of LPP, NPE, LLTSA, and DTE, the number of principle components is set as 150. The dimension steps are set to be 5 in final low-dimensional subspaces obtained by the 5 methods. After feature extraction, a nearest-neighbor classifier is employed for classification. The maximal average recognition rates of each method and the corresponding dimensions are shown in Table 3. The recognition rate curves versus the variation of dimensions are shown in Fig. 4.

From Table 2, we can see first that DTE significantly outperforms other methods and second that as unsupervised methods, DTE is more robust than the compared methods when there are different facial expressions and lighting conditions, irrespective of the variations in training sample size and dimensions. These two points are consistent with the experimental results presented in Sect. 4.1. The reason may be that the local geometric structure and local transition processes can reflect or predict the relationship with the different lighting, time, and expression samples in the text set in a certain sense. Thus, DTE is superior to the other methods in terms of recognition rates.

#### 4.3 Experiments on the polyU FKP database

PolyU FKP ( <http://www.comp.polyu.edu.hk/~biometrics/FKP.htm> ) images were collected from 165 volunteers, including 125 men and 40 women. Among them, 143 subjects were 20~30 years old and the others were 30~50 years old. Samples were collected in two separate sessions. In each session, the subject was asked to provide 6 images for each of the left index finger, the left middle finger, the right

**Table 2** The maximal average recognition rates (percent) of five methods on the AR face database and the corresponding dimensions (shown in parentheses) when 2, 3, 4, 5, and 6 samples per class are randomly selected for training and the remaining for test

#/class	2	3	4	5	6
PCA	67.79(150) $\pm$ 4.43	71.833(150) $\pm$ 4.31	78.87(150) $\pm$ 3.99	79.84(150) $\pm$ 3.17	82.58(150) $\pm$ 3.64
LPP	72.45(140) $\pm$ 4.01	76.39(130) $\pm$ 3.54	84.39(130) $\pm$ 4.07	88.68(110) $\pm$ 2.93	89.67(110) $\pm$ 2.32
NPE	71.39(150) $\pm$ 4.29	75.52(120) $\pm$ 3.53	84.14(135) $\pm$ 3.88	88.31(145) $\pm$ 3.14	89.17(140) $\pm$ 2.87
LLTAS	67.20(150) $\pm$ 4.91	76.60(150) $\pm$ 3.97	85.46(150) $\pm$ 3.45	87.30(150) $\pm$ 3.02	91.03(115) $\pm$ 2.79
DTE	74.68(150) $\pm$ 3.74	80.38(150) $\pm$ 2.95	88.37(150) $\pm$ 2.05	90.46(150) $\pm$ 2.37	93.05(150) $\pm$ 1.83

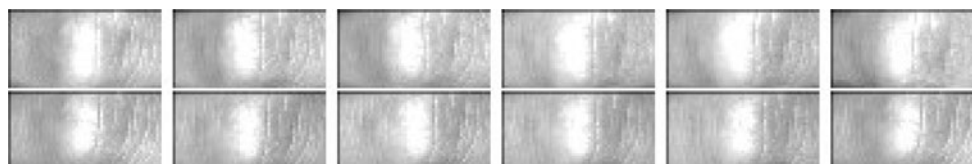


**Fig. 5** Sample images of one subject on the PolyU FKP database. The first line and the second line images were taken in different sections



**Table 3** The maximal recognition rates (percent) of five methods on the PolyU FKP database and the corresponding dimensions

Methods	PCA	LPP	NPE	LLTSA	DTE
Recognition rates	34.14	53.45	56.89	54.46	61.34
Dimensions	95	100	95	85	65

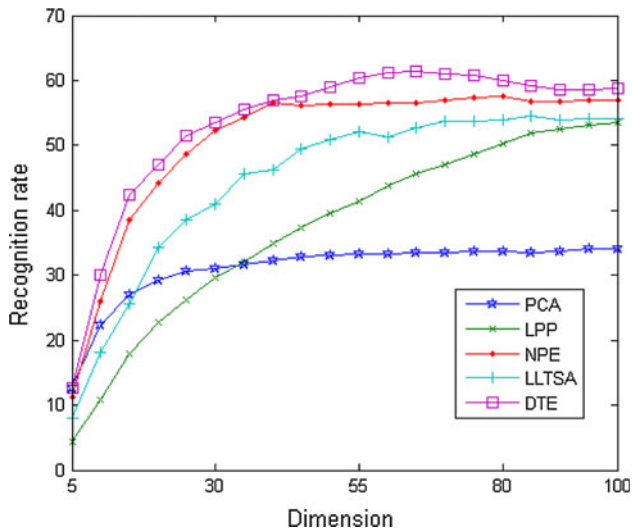


**Fig. 6** The maximal recognition rates (%) versus the dimensions on the PolyU FKP database

index finger, and the right middle finger. Therefore, 48 images from 4 fingers were collected from each subject. In total, the database contains 7,920 images from 660 different fingers. The average time interval between the first and the second sessions was about 25 days. The maximum and minimum intervals were 96 days and 14 days, respectively. For more details, please see [31, 33]. Some sample images

of one subject on the PolyU FKP database are shown in Fig. 5.

In the experiment, the extracted ROI images using ROI extraction algorithm described in [32] were used. We selected the first 6 images (01~06) of the left index finger captured in the first session as training samples, and the other 6 images (07~12) captured in the latter session as test samples. In the PCA phase of LPP, NPE, LLTSA, and DTE, the number of principle components is set as 100. The dimension steps are set to be 5 in final low-dimensional subspaces obtained by the 5 methods. The recognition rates are shown in Table 3. The recognition rate curves versus the variation of dimensions are shown in Fig. 6. As it can be seen from the Table 3 and Fig. 6, the recognition rate of DTE is also higher than the other methods'. This experiment shows that DTE is more robust than the other methods in time variations.

#### 4.4 Experiments on the PolyU-NIR face database

The released PolyU-NIR face database ([http://www4.comp.polyu.edu.hk/~biometrics/polyudb\\_face.html](http://www4.comp.polyu.edu.hk/~biometrics/polyudb_face.html)) contains images from 350 subjects, each contributing about 100 samples with variations of pose, expression, focus, scale, and time, etc. In total, 35,000 samples were collected in the database. The facial portion of each original image is automatically cropped according to the location of the eyes. The cropped face is then normalized to 64 × 64 pixels. The images of one sample are shown in Fig. 7. For more details, please see the webpage and [34].

In our experiments, a subset that contains 1,000 (20 × 50 = 1,000) images from 50 subjects and each subject provides 20 images was selected and used. Two images per subject were randomly selected as the training



**Fig. 7** Sample images of one subject on PolyU-NIR face database

**Table 4** The maximal recognition rates (percent) of five methods on the PolyU-NIR face database and the corresponding dimensions and standard deviations

Methods	PCA	LPP	NPE	LLTSA	DTE
Recognition rates	78.42 ± 1.99	82.07 ± 1.47	82.31 ± 1.35	79.42 ± 2.76	86.72 ± 2.12
Dimensions	99	90	99	99	99

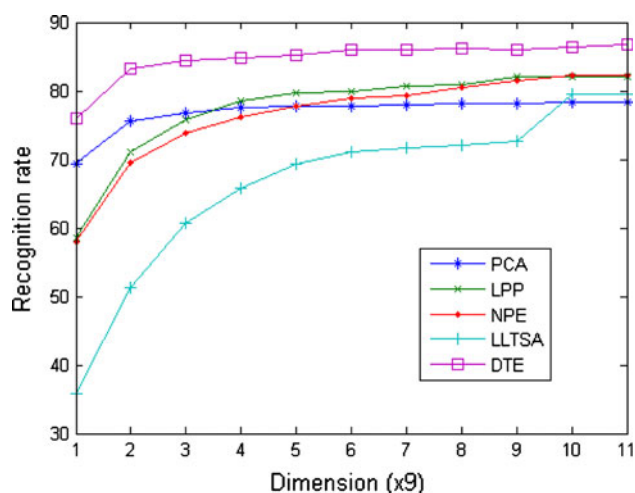


**Fig. 8** The average recognition rates (%) versus the dimensions on the PolyU-NIR face database

set and the remaining as the test set. The experiments were run 10 times. The dimension step is set to be 9. The recognition rates and the corresponding dimensions and standard deviations of each method are shown in Table 4. The recognition rate curves versus the variation of dimensions are shown in Fig. 8. As can be seen from the Table 4 and Fig. 8, DTE still perform better than the other methods. This indicates that the dynamic transition progresses do explore a more essential geometry structure of the data set for recognition task.

## 5 Conclusions

In this paper, we develop an unsupervised learning technique, called dynamic transition embedding (DTE), for dimensionality reduction of high-dimensional data. DTE models the data as a transition evolution progresses in different timescale and gives explicit feature extraction maps. The main idea of the DTE framework is that running the Markov chain forward (or equivalently taking larger powers of transition Markov matrices) will allow us to integrate the local geometry and, therefore, will reveal relevant geometric structures of the data set at different timescales. Assuming that data points are randomly sampled from an underlying low-dimensional manifold embedded in the ambient space, DTE projections can obtain the optimal linear projections based on transition probabilities reconstruction processes. Since the local structure and the transition progresses contain useful information, DTE can discover the intrinsic geometric information hidden within the data set, which is helpful for discrimination. The experimental results on Yale and AR face databases, the PolyU FKP database and PolyU-NIR

face database show that DTE consistently outperforms the well-known linear dimensionality reduction methods such as PCA, LPP, NPE, and LLTSA.

**Acknowledgments** This work is partially supported by the National Science Foundation of China under grant No. 60503026, 60632050, 60473039, 60873151, 61005005 and Hi-Tech Research and Development Program of China under grant No.2006AA01Z119.

## References

- Jain AK, Duin RPW, Mao J (2000) Statistical pattern recognition: a review. *IEEE Trans Pattern Anal Mach Intell* 22(1):3–4
- Jolliffe I (1986) *Principal component analysis*. Springer, New York
- Fukunnaga K (1991) *Introduction to statistical pattern recognition*, 2nd edn. Academic Press, New York
- Martinez AM, Kak AC (2001) PCA versus LDA. *IEEE Trans Pattern Anal Mach Intell* 23(2):228–233
- Belhumeur PN, Hespanha JP, Kriegman DJ (1997) Eigenfaces vs fisherfaces: recognition using class specific linear projection. *IEEE Trans Pattern Anal Mach Intell* 19(7):711–720
- Schölkopf B, Smola A, Muller KR (1998) Nonlinear component analysis as a Kernel eigenvalue problem. *Neural Comput* 5(10):1299–1319
- Yang J, Frangi AF, Zhang D, Yang J-y, Zhong J (2005) KPCA plus LDA: a complete kernel fisher discriminant framework for feature extraction and recognition. *IEEE Trans Pattern Anal Mach Intell* 27(2):230–244
- Tenenbaum JB, desilva V, Langford JC (2000) A global geometric framework for nonlinear dimensionality reduction. *Science* 290:2319–2323
- Roweis ST, Saul LK (2000) Nonlinear dimensionality reduction by locally linear embedding. *Science* 290:2323–2326
- Belkin M, Niyogi P (2001) Laplacian eigenmaps and spectral techniques for embedding and clustering. In: *Proceedings of advances in neural information processing system*, vol 14, Vancouver, Canada, December
- Belkin M, Niyogi P (2003) Laplacian eigenmaps for dimensionality reduction and data representation. *Neural Comput* 15:1373–1396
- Zhang Z, Zha H (2004) Principal manifolds and nonlinear dimensionality reduction via tangent space alignment. *SIAM J Sci Comput* 26(1):313–338
- Lafon S, Lee AB (2006) Diffusion maps and coarse-graining: a unified framework for dimension reduction, graph partitioning, and data set parameterization. *IEEE Trans Pattern Anal Mach Intell* 28(9):1393–1403
- Donoho D, Grimes C (2003) Hessian eigenmaps: new locally linear embedding techniques for high-dimensional data. *Proc Nat Acad Sci* 100(10):5591–5596
- Lin T, Zha H, Lee S (2008) Riemannian manifold learning. *IEEE Trans Pattern Anal Mach Intell* 30(5):796–809
- He X, Cai D, Yan S, Zhang H (2005) Neighborhood preserving embedding. In: *Proceedings in international conference on computer vision (ICCV)*, Beijing, China
- He X, Niyogi P (2003) Locality preserving projections. In: *Proc. 16th conf. neural information processing systems*
- Zhang T, Yang J, Zhao D, Ge X (2007) Linear local tangent space alignment and application to face recognition. *Neurocomputing* 70:1547–1553
- Chen H-T, Chang H-W, Liu T-L (2005) Local discriminant embedding and its variants. In: *Proc. IEEE conf. computer vision and pattern recognition* 2:846–853

20. Yan S, Xu D, Zhang B, Zhang H-J, Yang Q, Lin S (2007) Graph embedding and extensions: a general framework for dimensionality reduction. *IEEE Trans Pattern Anal Mach Intell* 29(1):40–51
21. Fu Y, Yan S, Huang TS (2008) Classification and feature extraction by simplexization. *IEEE Trans Inf Forensics Secur* 3(1):91–100
22. Bo L, De-Shuang H, Chao W, Kun-Hong L (2008) Feature extraction using constrained maximum variance mapping. *Pattern Recogn* 41(11):3287–3294
23. Zhi R, Ruan Q (2007) Facial expression recognition base on two-dimensional discriminant locality preserving projections. *Neurocomputing* 70:1543–1546
24. Wan M, Lai Z, Shao J, Jin Z (2009) Two-dimensional local graph embedding discriminant analysis (2DLGEDA) with its application to face and palm biometrics. *Neurocomputing* 73:193–203
25. Xu Y, Feng G, Zhao Y (2009) One improvement to two-dimensional locality preserving projection method for use with face recognition. *Neurocomputing* 73:245–249
26. Nadler B, Lafon S, Coifman RR, Kevrekidis IG (2006) Diffusion maps spectral clustering and eigenfunctions of Fokker-Planck operators. *Adv Neural Inf Process Syst* 18:955–962
27. Lafon S (2004) Diffusion maps and geometric harmonics. Ph. D. dissertation, Yale University
28. Hein M, Audibert J, von Luxburg U (2005) From graphs to manifolds—weak and strong pointwise consistency of graph Laplacians. *Lect Notes Comput Sci* 3559:470–485
29. Luxburg U (2007) A tutorial on spectral clustering. *Stat Comput* 17:395–416
30. Coifman RR, Lafon S, Lee AB, Maggioni M, Nadler B, Warner F, Zucker SW (2005) Geometric diffusions as a tool for harmonic analysis and structure definition of data: diffusion maps. In: *Proceedings of the National Academy of Sciences* 102(21):7426–7431
31. Zhang L, Zhang L, Zhang D, Zhu H (2011) Ensemble of local and global information for finger-knuckle-print recognition. *Patt Recogn*, accepted
32. Zhang L, Zhang L, Zhang D, Zhu H (2010) Online finger-knuckle-print verification for personal authentication. *Patt Recogn* 43(7):2560–2571
33. Zhang L, Zhang L, Zhang D (2009) Finger-knuckle-print: a new biometric identifier. In: *Proceedings of the IEEE international conference on image processing*
34. Zhang B, Zhang L, Zhang D, Shen L (2010) Directional binary code with application to PolyU near-infrared face database. *Patt Recogn Lett* 31(14):2337–2344